Journal of Hepatocellular Carcinoma

Dovepress
Taylor & Francis Group

Open Access Full Text Article

ORIGINAL RESEARCH

ARID3A Promotes Tumor Progression by Activating TNF-α/NF-κB Signaling in Dual-Phenotype Hepatocellular Carcinoma

Minjun Li[1,2,*], Taixin Yang[1,*], Juntao Huang[1], Xinyuan Wu[1], Jingyu Chen[1], Jindu Li[1], Binglin Shi[3], Jie Zhang[1], Bangde Xiang[1,2]

[1]Department of Hepatobiliary Surgery, Guangxi Medical University Cancer Hospital, Nanning, Guangxi, People's Republic of China; [2]Key Laboratory of Early Prevention and Treatment for Regional High Frequency Tumor, Ministry of Education, Nanning, Guangxi, People's Republic of China; [3]Department of General Surgery, Fangchenggang First People's Hospital, Fangchenggang, Guangxi, People's Republic of China

*These authors contributed equally to this work

Correspondence: Bangde Xiang; Jie Zhang, Email xiangbangde@gxmu.edu.cn; zhangjie1@gxmu.edu.cn

Objective: Dual-phenotype hepatocellular carcinoma (DPHCC) is a unique subtype of hepatocellular carcinoma (HCC) characterized by strong tumor stemness and invasive capabilities. ARID3A is identified as a potential regulator of tumor stemness in DPHCC by applying transcriptomic analysis. The precise mechanisms of ARID3A on the aggressive behavior of DPHCC remain to be further explored.

Materials and Methods: In vitro functional experiments and in vivo tumorigenesis assays were used to validate the malignant behaviors of ARID3A. RNA sequencing was performed on ARID3A-transfected cells to identify ARID3A-mediated regulatory mechanisms. Finally, the impact of ARID3A–TNF-α/NF-κB axis on HCC malignant behavior was analyzed through in vitro blocking or stimulation experiments.

Results: The expression of ARID3A was upregulated in DPHCC and was associated with poor prognosis among these patients (p = 0.006, HR = 3.77, 95% CI:1.762–8.069). In vitro and in vivo experiments indicated that ARID3A facilitated stemness features and tumor progression. Findings from RNA-seq suggested that ARID3A enhanced tumor stemness and activated epithelial-mesenchymal transition through the activation of TNF-α-mediated NF-κB signaling. In vitro stimulation of ARID3A-transfected cells lines with recombinant TNF-α protein or inhibition of TNF-α-mediated NF-κB signaling regulated the ARID3A-mediated invasiveness.

Conclusion: Our study reveals that ARID3A acts as an oncogene and promotes aggressive features of stem-like cells in DPHCC via the ARID3A–TNF-α/NF-κB axis. Thus, it may facilitate the development therapeutic strategy for DPHCC.

Keywords: dual-phenotype HCC, ARID3A oncogene, inflammatory signaling

Introduction

Hepatocellular carcinoma (HCC) is a highly heterogeneous malignancy, and its treatment efficacy remains unsatisfactory even after curative therapies.[1] One important reason is that cancer stem cells (CSC) play an important role in promoting the self-renewal and invasion capacities, leading to tumor relapse and threatening the long-term survival of HCC patients.[2] Of note, dual-phenotype hepatocellular carcinoma (DPHCC) is a unique subtype of HCC with CSC characteristics. Unlike combined hepatocellular and intrahepatic cholangiocarcinoma (cHCC-ICC), DPHCC only shows typical HCC morphological features, and is characterized by the partial co-expression of hepatocyte and cholangiocyte markers, such as cytokeratin 19 (CK19).[3] While CK19 is also deemed as a stemness marker, and CK19 positive HCC is associated with highly aggressive biological behaviors including vascular invasion and lymph node metastasis.[4,5] Similarly, patients with DPHCC have a significantly worse prognosis than those with non-DPHCC and exhibit stronger stemness features in

Received: 25 June 2025
Accepted: 5 November 2025
Published: 19 November 2025

the tumor tissue.[3] These findings suggest that DPHCC is regarded as a CSC phenotype and is worthwhile for investigating the regulatory mechanisms of CSCs in DPHCC. The presence and maintenance of CSC often involves the activation of oncogenic pathways, such as the Wnt/β-catenin and NF-κB signaling pathways, which could be induced by transcriptional regulators such as transcription factors.[6–8] More importantly, the activation of these pathways in CSC may acquire metastatic potential by triggering the epithelial-mesenchymal transition (EMT) programme, thereby facilitating the distant metastasis of tumors.[9,10]

ARID3A is a member of the AT-rich interaction domain (ARID) family that encodes a DNA-binding protein. It is involved in cell cycle control, transcriptional regulation, and possibly chromatin structural modifications.[11,12] The important role of elevated expression of ARID3A in promoting stemness properties and invasiveness in several malignancies and also contributes to poor prognosis in these patients.[13,14] In addition, High ARID3A expression in malignancy may enhance the embryonic stem cell characteristics of tumor cells and promote invasion and metastasis.[13] In HCC, ARID3A was also found to be a cooperative transcription factor that regulate the stemness signature,[15] and its high expression in HCC correlated with poor prognosis.[16]

In the present study, we revealed that ARID3A is upregulated in DPHCC using transcriptional sequencing and tissue expression analysis. However, it remains to be further investigated what may trigger the activation of ARID3A in CSC-like HCC phenotype–DPHCC, and whether the transcriptional activation pathways influence the CSC properties of DPHCC. Importantly, we identified the ARID3A–TNF-α/NF-κB axis is important for maintaining the CSC properties and invasive phenotype and investigated the potential mechanism between inflammatory signaling and tumor stemness in DPHCC.

Materials and Methods

Patients and Samples

HCC patients who received curative hepatic resection as primary treatment at Guangxi Medical University Cancer Hospital between 2018 and 2019 were recruited for this study. Those who experienced tumor relapse within 1 month after resection were excluded. Tumor samples were collected from resected tissues and properly preserved. Postoperative pathological examinations were routinely conducted, and HCC was diagnosed by experienced pathologists. Patients were routinely follow-up every 6 months after initial resection. This study was conducted in accordance with the Declaration of Helsinki, and preoperative written informed consents were obtained from all patients.

RNA-Sequencing

The RNA sequencing (RNA-seq) of HCC cohort was performed by Wuxi NextCODE (Shanghai, China). A detailed RNA-seq procedure has been described in our previous work.[17] The ARID3A overexpression and knockdown HCC cell lines were also collected and transferred to Genergy Biotechnology (Shanghai, China) for RNA-seq. The principal procedures of cell sequencing were similar to those of HCC cohort and were briefly described as follows: Total RNA was extracted from lentivirus-transfected cells, followed by sample quality control, library construction and sequencing. The reads of these samples were compared against the reference human genome (version Hg38) using the STAR software.

Immunohistochemistry

Tumor sections from patients in the RNA-seq cohort were collected to perform immunohistochemical (IHC) staining to evaluate ARID3A expression in DPHCC and non-DPHCC tissues. IHC staining and section evaluation were performed in accordance with the protocol described in our previous study.[17] For IHC staining, ARID3A (1:500 dilution, Proteintech) was used as the primary antibody.

Cell Culture and Lentivirus-Transfection

The Huh7, Hep3B, and SNU449 HCC cell lines were selected for the in vitro and in vivo experiments. The cell lines were cultured in DMEM or RPMI1640 medium supplemented with 10% fetal bovine serum (FBS). The cells were incubated at 37 °C with 5% CO_2. ARID3A overexpression and knockdown lentiviral vectors were assembled by

Genechem Corporation (Shanghai, China). Lentivirus transfection was conducted in accordance with provided protocol. Huh7 and Hep3B cells were transfected with ARID3A knockdown lentivirus (MOI = 5) and SNU449 cells were transfected with ARID3A overexpression lentivirus (MOI = 20). Empty lentivirus vectors were also transfected into these cell lines as controls. These HCC cell lines were transfected with lentivirus for 16–24 hours and selected with resistance medium supplemented with 2.0–5.5 μg/mL puromycin for at least 7 days. The transfection efficiency was validated by quantitative polymerase chain reaction (qPCR) and Western blot (WB).

Wound Healing Assay

Cell suspensions were collected and seeded into six-well plates for culture. The medium was removed after the cells reached full confluence. Then, we used a 200μL sterile pipette tip to create a scratch, followed by washing with phosphate-buffered saline (PBS). The cells were cultured in serum-free medium at 37 °C, and images were captured at 0 and 24 hours. The percentage of wound closure was calculated using the following formula: (original wound area − actual wound area)/original wound area × 100.

Migration and Invasion Assays

This experiment was conducted in 24-well transwell chambers. The invasion chambers were loaded with 50μL Matrigel (Corning, USA) diluted at a 1:8 ratio in serum-free DMEM or RPMI 1640 medium. The cell suspension was diluted to 3×10^5 cells/mL using serum-free medium and 100μL was added to a transwell chamber. For the migration assay, the cell suspension was added to the transwell chamber without Matrigel. After 24 to 72 hours of incubation, the cells were fixed with 4% paraformaldehyde for 30 minutes and stained with 0.1% crystal violet.

Cell Counting Kit and Colony Formation Assays

The cells were seeded at a density of 3×10^3 cells per well in 96-well plates. The cell counting kit-8 (CCK-8) reagent (Vazyme, China) was added to the wells and incubated at 37 °C for 3 hours. Absorbance was measured at 450 nm after 0, 24, 48 and 72 hours. For the cloning formation assay, cells were seeded in six-well plates with complete medium and incubated for approximately three weeks. Each 6-well plate was fixed with 4% paraformaldehyde for 30 minutes and then stained with 0.1% crystal violet.

Spheroid Formation Assay

Huh7 and Hep3B cells were seeded at a density of 5×10^3 cells/mL in ultra-low attachment six-well plates (Corning, USA) using DMEM supplemented with 1:50 diluted B27, 20ng/mL epidermal growth factor and 20ng/mL fibroblast growth factor (Invitrogen, USA). The number and size of the spheroids were recorded after 7 days of incubation.

Immunofluorescence

DPHCC and non-DPHCC were identified using multiplex immunofluorescence (mIF) based on the co-expression of hepatocyte (HepPar1, Glypican3, and Arginase1) and cholangiocyte (CK19, CK7, and MUC1) markers in HCC samples. The procedure for the mIF assay is described in our previous study.[18] The cell immunofluorescence assay was carried out as follows: cells were washed with PBS and fixed with permeabilize solution for 20 minutes. Subsequently, the cell slides were blocked with 3% BSA solution for 30 minutes, followed by incubating with primary antibody at 4 °C overnight. After washing with PBS, the cell slides were incubated with secondary antibody at room temperature for 50 minutes and cell nuclei were stained with DAPI, and fluorescence microscopy was used to detect the fluorescence intensity of NF-κB in cells.

In vivo Tumorigenesis Assay

Huh7 and Hep3B cells were transfected with SH-ARID3A and SH-NC lentiviral vectors. Then cells were suspended in 100μL of PBS and subcutaneously injected into the right flank of 5-week-old BALB/C nude mice (3×10^6 cells per mouse). The tumor size of these mice was measured every four days, and the mice were sacrificed after 16–28 days of observation. Tumor volumes were calculated using the following formula: volume = (width^2×length)/2.

RNA Extraction and qPCR

Total RNA from lentivirus-transfected cells was extracted using the TRIzol reagent method, and cDNA was reverse-transcribed using a reverse transcription reagent (Vazyme, China). The qPCR system consisted of SYBR dye, cDNA and primers. The qPCR program was carried out on a QuantStudio5 PCR system (Applied Biosystems, USA). Primer specificity was validated using melt curve analysis. ARID3A and endogenous control primers were obtained from Sangon Biotech (Shanghai, China), and the primer sequences were as follows: ARID3A forward: 5'-ACCACGGCGACTGGACTTA-3'; reverse: 5'-CACAGGTGTCCCTCGCTTC-3'. GAPDH forward: 5'-CGCTCTCTGCTCCTCCTGTT-3'; reverse:5'-CCATGGTGTCTGAGCGATGT-3'. The mRNA expression levels of ARID3A were calculated using relative quantification ($2^{-\Delta\Delta Ct}$).

Western Blot

Total protein was extracted using RIPA lysis buffer mixed with protease inhibitor (Beyotime, China). In addition, ARID3A lentivirus-transfected Huh7 and Hep3B cells were treated with 40 ng/mL recombinant human TNF-α protein (Servicebio, China) for 8 hours. SNU449 cells were treated with 10μM/mL of NF-κB inhibitor–NF-κB-IN-11 (MCE, USA) for 8 hours. Then these cells were also collected to extract total protein for the WB assay. Protein samples were electrophoresed on a 6–10% polyacrylamide gel (Epizyme Biotech, China) and subsequently transferred to a PVDF membrane (Merck Millipore, USA). Antibodies against E-cadherin, N-cadherin, Snail1, ARID3A, NF-κB, CK19, CD133, TNF-α, GAPDH or β-actin antibodies. After incubation with goat anti-rabbit secondary antibodies for 1 hour, the PVDF membranes were visualized using an Odyssey scanning system (LI-COR Biosciences, USA). Detailed information about dilution ratio of primary and secondary antibodies were supplemented in Table S1.

Statistical Analysis

All experimental data were analyzed using GraphPad Prism 9.0 and are presented as mean ± standard deviation. Continuous variables were analyzed using Wilcoxon rank sum test, Student's *t* test or analysis of variance (ANOVA). Categorical variables were compared using Pearson's χ^2 test or Fisher's exact test. Survival analyses were performed using the Kaplan–Meier method with the Log rank test. All bioinformatic analyses were conducted using Rstudio (Version 4.1.2, The R Foundation, Vienna, Austria). Differentially expressed genes (DEGs) were designated with expression levels higher than | log (fold change) | > 1 and p values < 0.05. Protein–protein interaction analysis was carried out on the DEGs to screen the top interactive genes. Weighted gene co-expression network analysis (WGCNA) was performed to identify the DPHCC-related genes. Kyoto Encyclopedia of Genes and Genomes (KEGG) analysis was conducted to identify potential regulatory pathways. Gene ontology (GO) analysis was performed to explore the biological functions of the DEGs. Gene set enrichment analysis (GSEA) and hallmark gene set enrichment analyses were also used to analyze the enriched biological functions and signaling pathways of DEGs. Statistical significance was defined as $P < 0.05$.

Results

ARID3A is Upregulated in DPHCC and Correlated with Poor Prognosis

Eighty-three patients with HCC were enrolled in the cohort. Baseline characteristics of the RNA-seq cohort were shown in Table S2. We identified 19 DPHCC and 64 non-DPHCC patients using the mIF staining (Figure 1). RNA-seq was also performed on the HCC cohort. A total of 787 DEGs were identified between the DPHCC and non-DPHCC groups, consisting of 531 upregulated and 256 downregulated DEGs (Figure 2A). The complete list of DEGs was supplemented in Table S3. The volcano plot and protein–protein interaction analysis indicated that several stemness-related genes, including KRT19, EPCAM, CD133 (PROM1), CD24, and AFP, were highly enriched in DPHCC (Figure 2B and C). To investigate the potential regulators of strong stemness features in DPHCC, we further conducted WGCNA, and the MEsalmon and MEcyan modules were identified as DPHCC-related gene modules (Figure 2D). Gene ontology analysis of these module genes suggested that they were highly correlated with the transcriptional regulation process (Figure 2E). A total of 42 genes were screened by intersecting the DEGs and module genes, including ARID3A, HMGA2, SALL4 and etc (Figure 2F). Among these, ARID3A was highly

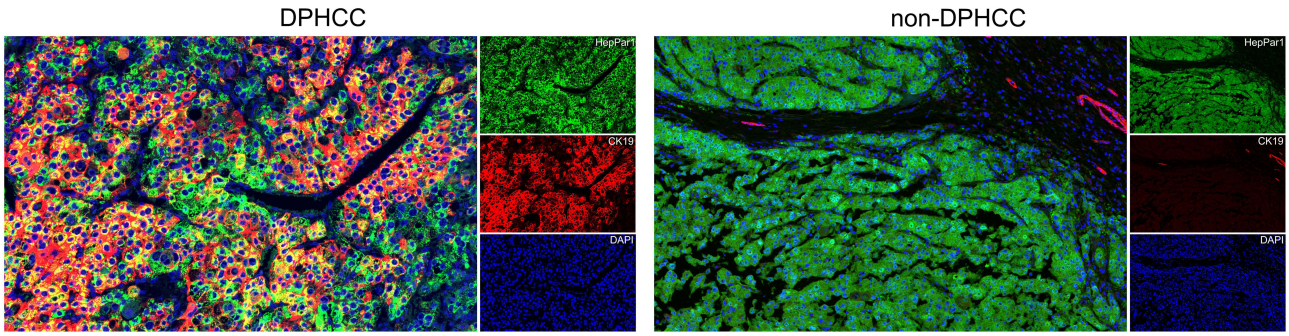

Figure 1 Representative multiplex immunofluorescence staining of DPHCC and non-DPHCC. The figure was enlarged by 200X.

correlated with transcriptional regulation and was selected for further validation. Survival analysis suggested that higher ARID3A expression exhibited a significantly worse prognosis ($p = 0.006$, HR = 3.77, 95% CI:1.762–8.069, Figure 2G). This result was further supported by the HCC cohort in The Cancer Genome Atlas (TCGA) project, which was visualized by the GEPIA website (http://gepia.cancer-pku.cn/index.html) ($p = 0.038$, Figure 2H). The mRNA expression level of ARID3A was significantly higher in the DPHCC group than that in the non-DPHCC group ($p < 0.001$, Figure 2I). Immunohistochemical staining further validated the upregulated expression of ARID3A in DPHCC tissues ($p = 0.027$, Figure 2J).

ARID3A Enhances the Migration and Invasion Capabilities of HCC

To explore the function of ARID3A in HCC, ARID3A shRNA vectors were stably transfected into Huh7 and Hep3B cell lines, whereas ARID3A overexpression vectors were transduced into SNU449 cells. The expression levels of ARID3A in these cell lines were determined by qPCR and WB (Figure 3A and B). Subsequently, functional assays were performed to elucidate the oncogenic potential of ARID3A. Both wound-healing and transwell assays demonstrated that ARID3A enhanced the migration ability of HCC cells. Specifically, inhibition of the expression of ARID3A decreased the migration rate of Huh7 and Hep3B cells, and enhanced migration ability of SNU449 cells ($p<0.05$, Figure 3C and D). The invasion assay also indicated that ARID3A significantly promoted HCC invasiveness of HCC ($p < 0.05$, Figure 3D).

Knockdown of ARID3A Suppresses Tumor Proliferation and Stemness

We also conducted colony formation and CCK-8 assays to evaluate the proliferative potential of ARID3A in HCC cell lines. Both colony formation and CCK-8 assays demonstrated that inhibition of ARID3A diminished the cell proliferative ability of Huh7 and Hep3B cells ($p < 0.05$). Intriguingly, no significant difference was observed in the proliferation capacity of SNU449 cells after ARID3A overexpression, compared with the empty vector control ($p > 0.05$, Figure 4A and B). This might be due to the variance of responsiveness of different cell lines after lentiviral transfection. Given that the RNA-seq analysis revealed that ARID3A was significantly upregulated in DPHCC and that DPHCC was characterized by the upregulation of multiple stemness-related markers, we conducted a WB assay to verify whether ARID3A is involved in regulating the tumor stemness of DPHCC. We found that DPHCC-related CSC markers, including CK19 and CD133, were significantly downregulated in Huh7 and Hep3B cells and upregulated in SNU449 cells, which was further confirmed by spheroid formation assays (Figure 4C and D). An in vivo tumorigenesis experiment was performed using Huh7 cells. Subcutaneous xenograft tumors were measured routinely and the mice were sacrificed after the observation period. The results indicated that the knockdown of ARID3A significantly inhibited the growth of xenograft tumors in BALB/C nude mice with subcutaneous injection of Huh7 and Hep3B cells ($p < 0.01$, Figure 4E).

ARID3A Regulates Tumor Stemness and EMT Through the TNF-α Mediated NF-κB Signaling

Since in vitro experiments demonstrated that ARID3A facilitated tumor migration and invasiveness, we further conducted RNA-seq on ARID3A-transfected cell lines to elucidate the potential regulatory mechanisms of ARID3A-

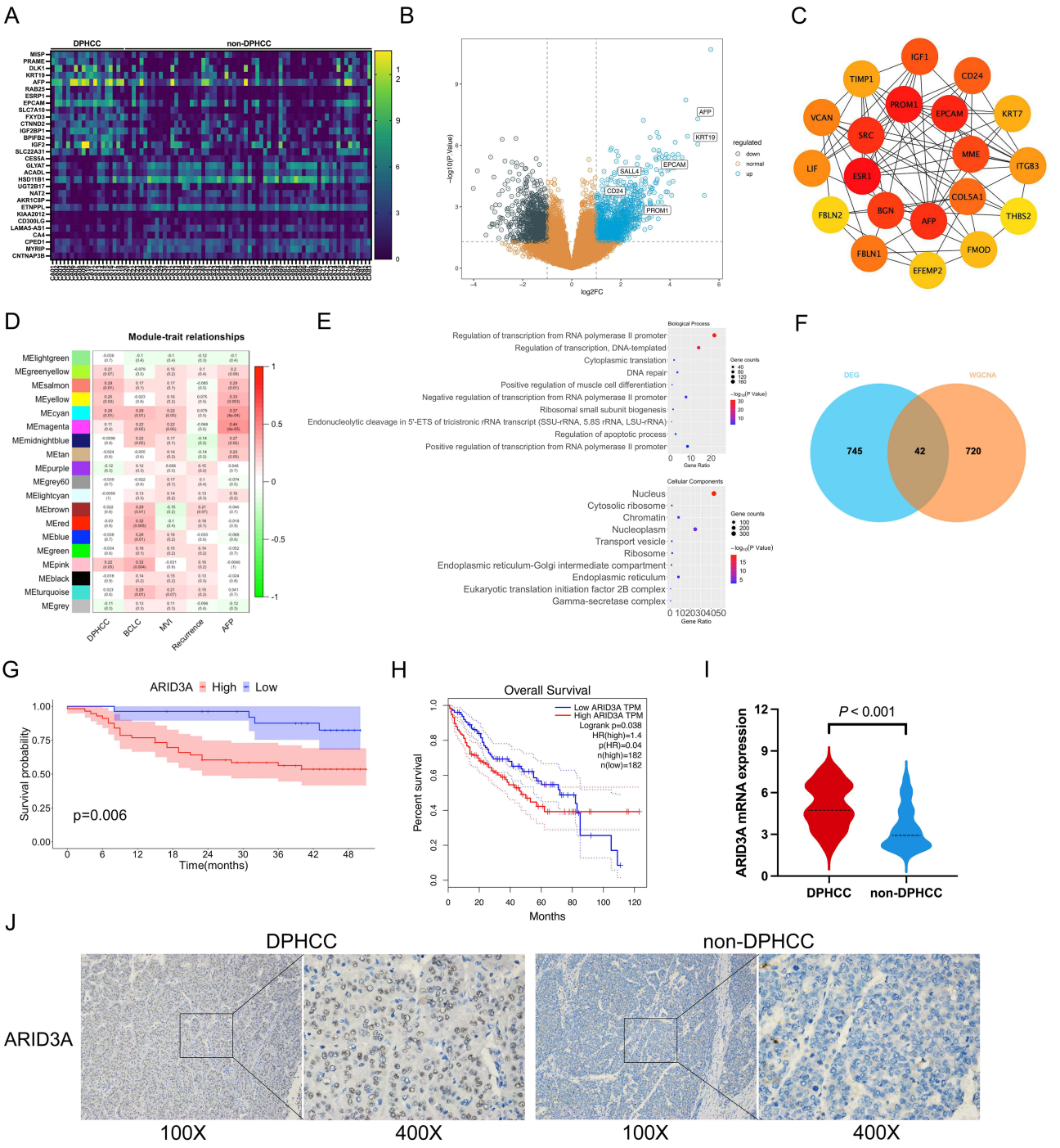

Figure 2 Identification and validation of ARID3A as a potential regulator of DPHCC.(**A**) Heatmap showed the top differentially expressed genes between DPHCC and non-DPHCC. (**B**) Volcano plot depicted the stemness features of DPHCC. (**C**) Protein–protein interaction analysis identified the stemness-related genes in DPHCC. (**D**) DPHCC-related gene modules were identified by weighted gene co-expression network analysis. (**E**) Gene ontology analysis of DPHCC-related gene modules was conducted. (**F**) Venn plot screened potential key regulators of DPHCC. (**G** and **H**) Survival analysis of ARID3A expression in the RNA-seq cohort and TCGA-LIHC cohort. (**I**) ARID3A mRNA expression level in the RNA-seq cohort was evaluated (n = 83) (**J**) Representative immunohistochemical staining of DPHCC and non-DPHCC groups was presented.

enhanced invasiveness and stemness in DPHCC. The gene expression profile is presented as a heatmap (Figure 5A). The DEGs of ARID3A-knockdown cell lines were selected for GO and KEGG analyses. The DEGs were enriched in the cell growth and nucleotide metabolic pathways (Figure 5B), which was in accordance with the in vitro experiments, indicating that knockdown of ARID3A suppressed the proliferation ability of HCC. KEGG analysis suggested that the

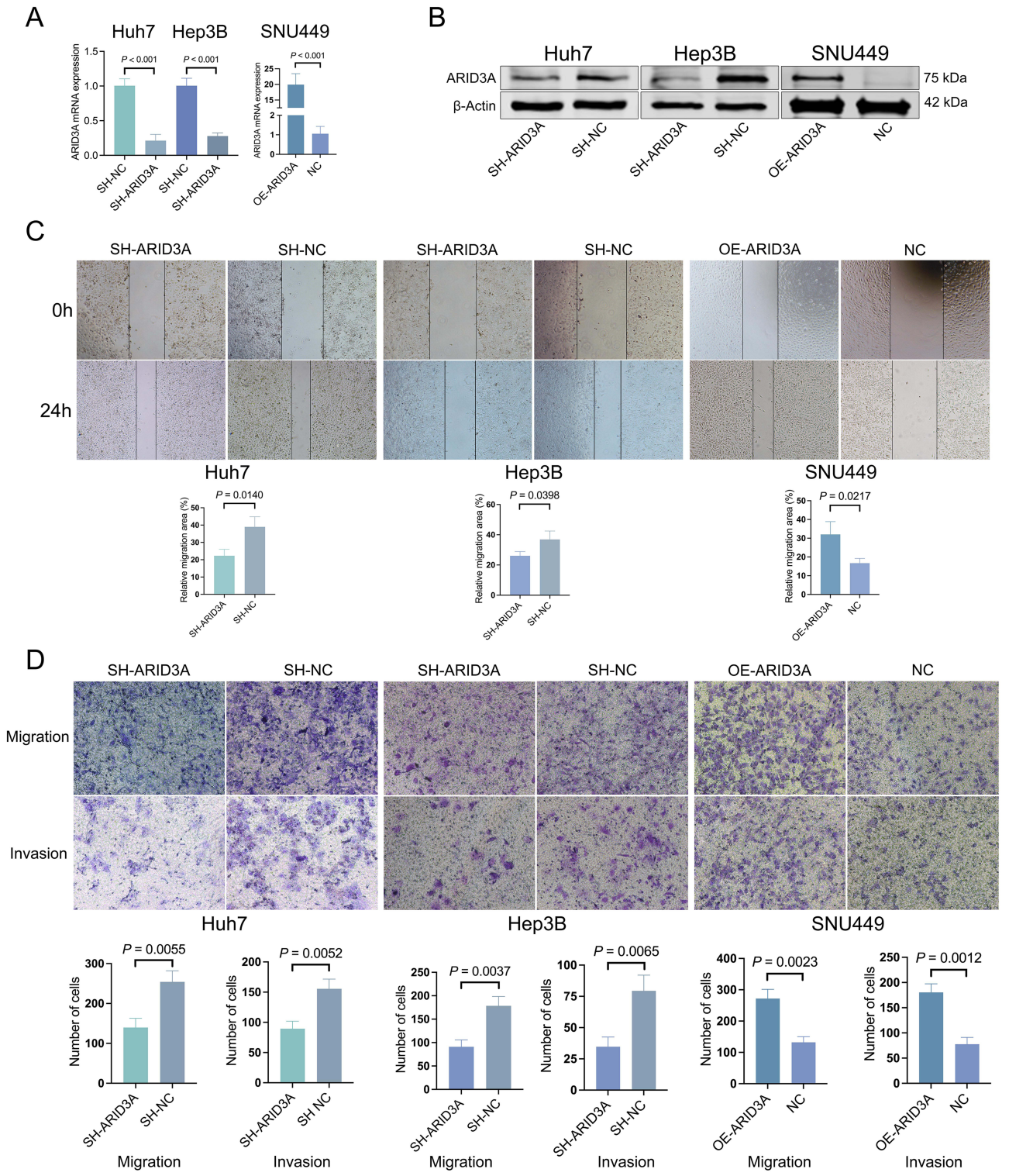

Figure 3 ARID3A enhances the migration and invasion potential of HCC.(**A** and **B**). The expression of ARID3A in lentivirus-transfected HCC cell lines was evaluated by QPCR and WB assays (n = 3). (**C**). Wound healing assay was used to detect the migration ability of HCC cells (n = 3). (**D**). The transwell method was used to conduct migration and invasion assays on HCC cells (n = 3).

https://doi.org/10.2147/JHC.S549213

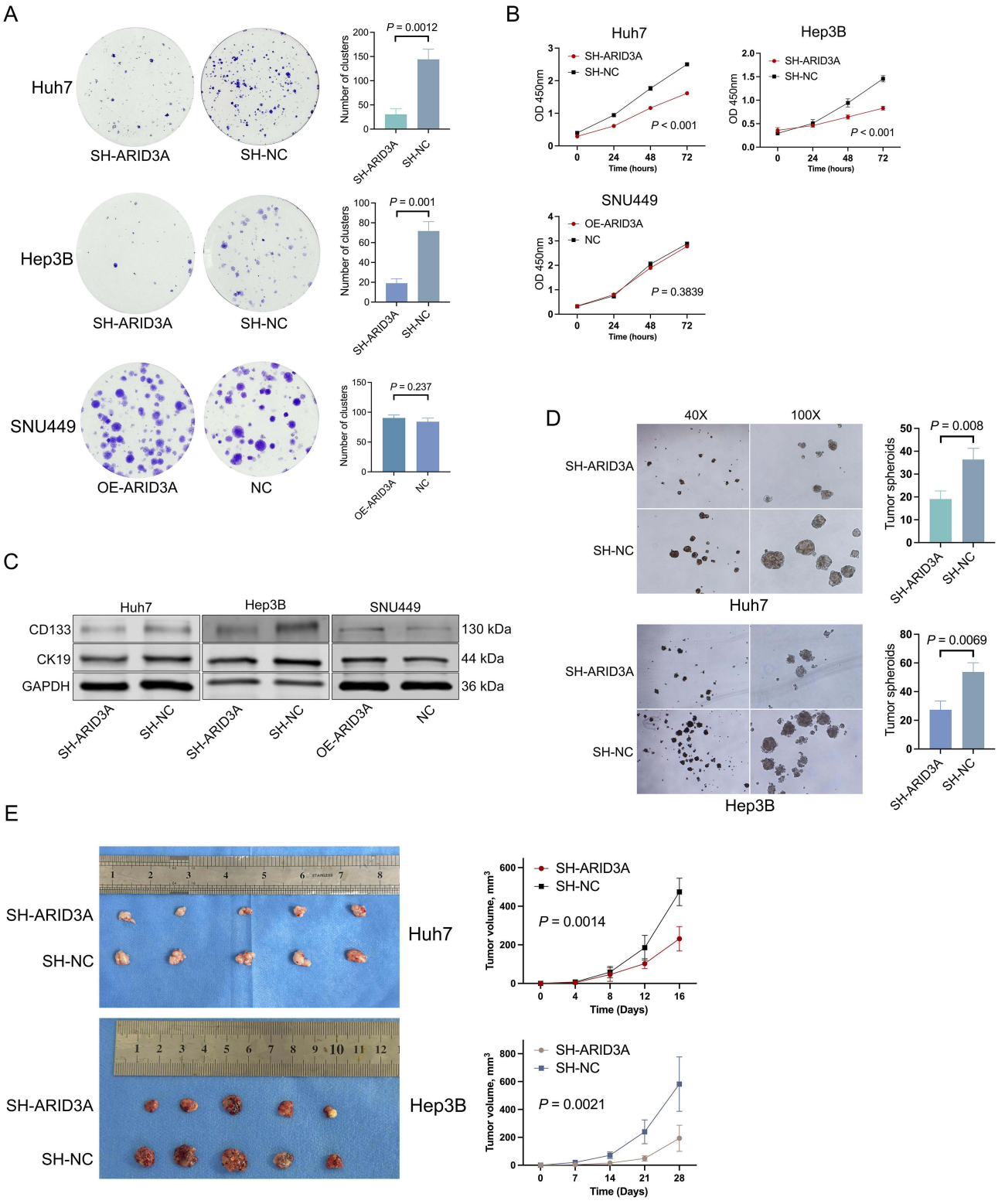

Figure 4 Inhibition of ARID3A suppresses cell growth and tumor stemness.(**A** and **B**). Colony formation and CCK-8 assays were carried out on HCC cells. (**C**). The expression levels of CK19 and CD133 were detected by WB assay in HCC cells. (**D**). Spheroid formation assay was performed on Huh7 and Hep3B cells to further evaluate the influence of ARID3A on the stemness properties of HCC cells. (**E**). A xenograft model was established with Huh7 and Hep3B cells.

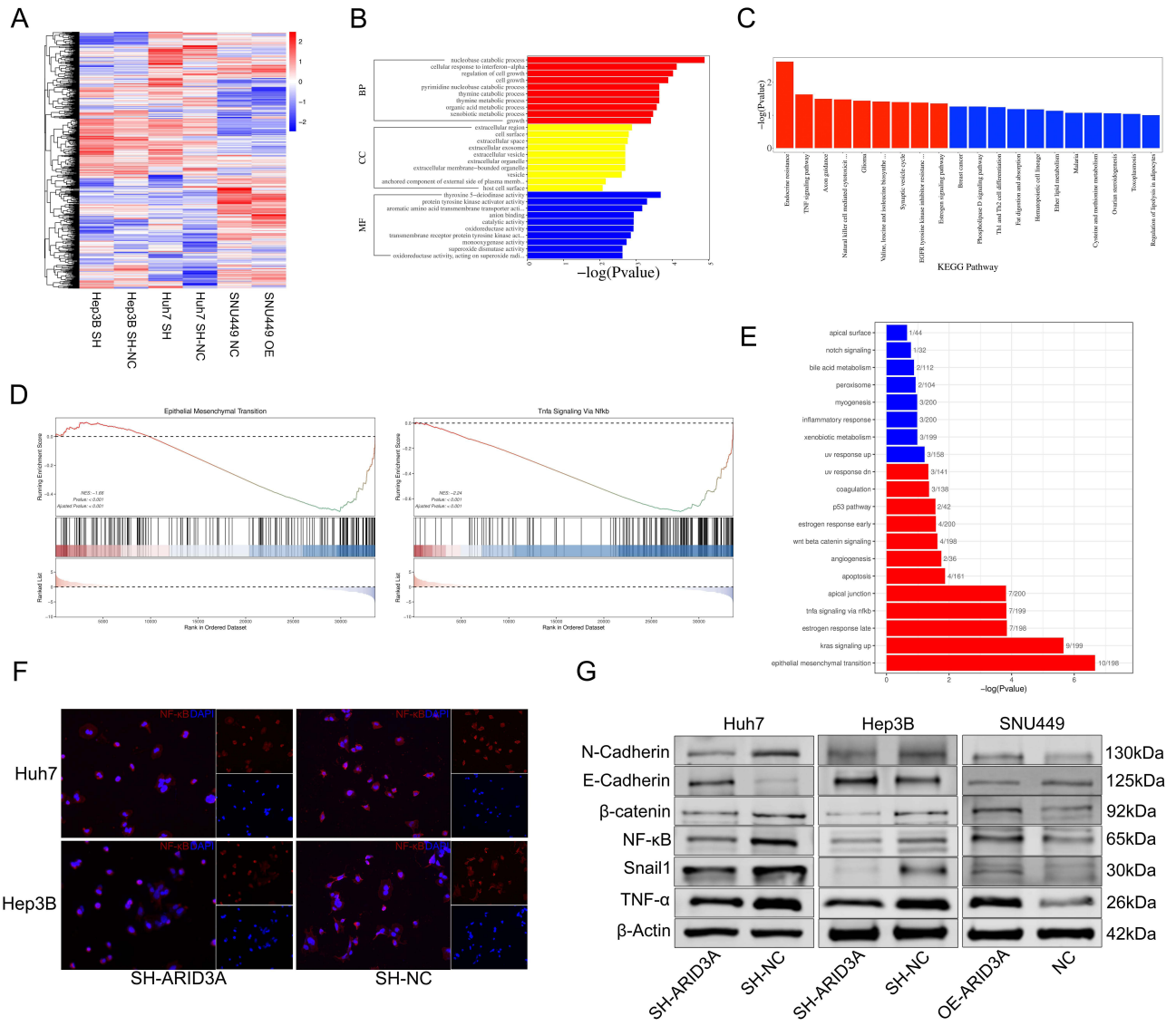

Figure 5 RNA-seq analysis and WB assay reveal that ARID3A involves in TNF-α-mediated NF-κB signaling.(**A**). Heatmap of lentivirus-transfected cell RNA-seq. (**B** and **C**). GO and KEGG analyses of the differentially expressed genes in ARID3A-transfected HCC cells. (**D** and **E**). GSEA and Hallmark enrichment analyses of ARID3A-knockdown HCC cells. (**F**). Immunofluorescence images of ARID3A-knockdown HCC cells, the figure was enlarged by 100X. (**G**). Western blot assay of EMT, NF-κB and Wnt/β-catenin pathways (n=3).

Abbreviations: EMT, epithelial-mesenchymal transition. GO, gene ontology; GSEA, gene set enrichment analysis. KEGG, Kyoto Encyclopedia of Genes and Genomes.

DEGs were involved in the TNF signaling pathway (Figure 5C). We further performed GSEA and hallmark enrichment analyses to explore the ARID3A-mediated regulatory mechanisms and found that the EMT, TNF-α/NF-κB, and Wnt/β-catenin signaling pathways were significantly downregulated in Huh7 and Hep3B cells (Figure 5D and E). This finding was further supported by immunofluorescence and WB assays, where the expression levels of NF-κB, β-catenin, and EMT-related markers Snail and N-cadherin were downregulated and E-cadherin was upregulated in Huh7 and Hep3B cells. Similar results were observed for SNU449 cells. Notably, TNF-α expression was also regulated by ARID3A (Figure 5F and G). Since we identified and validated that ARID3A regulated tumor stemness and EMT through TNF-α-mediated NF-κB signaling, we further conducted a WB assay to explore whether exogenous TNF-α treatment could induce ARID3A expression and regulate these phenotypic changes. First, wild-type Huh7 and Hep3B cells were treated with 40ng/mL recombinant TNF-α protein, and the expression level of ARID3A was upregulated after 8 hours of stimulation (Figure 6A). We further examined the expression levels of ARID3A, NF-κB, CSC, and EMT markers in lentivirus-transfected Huh7 and Hep3B cells after TNF-α treatment. The results also revealed that TNF-α partially

https://doi.org/10.2147/JHC.S549213

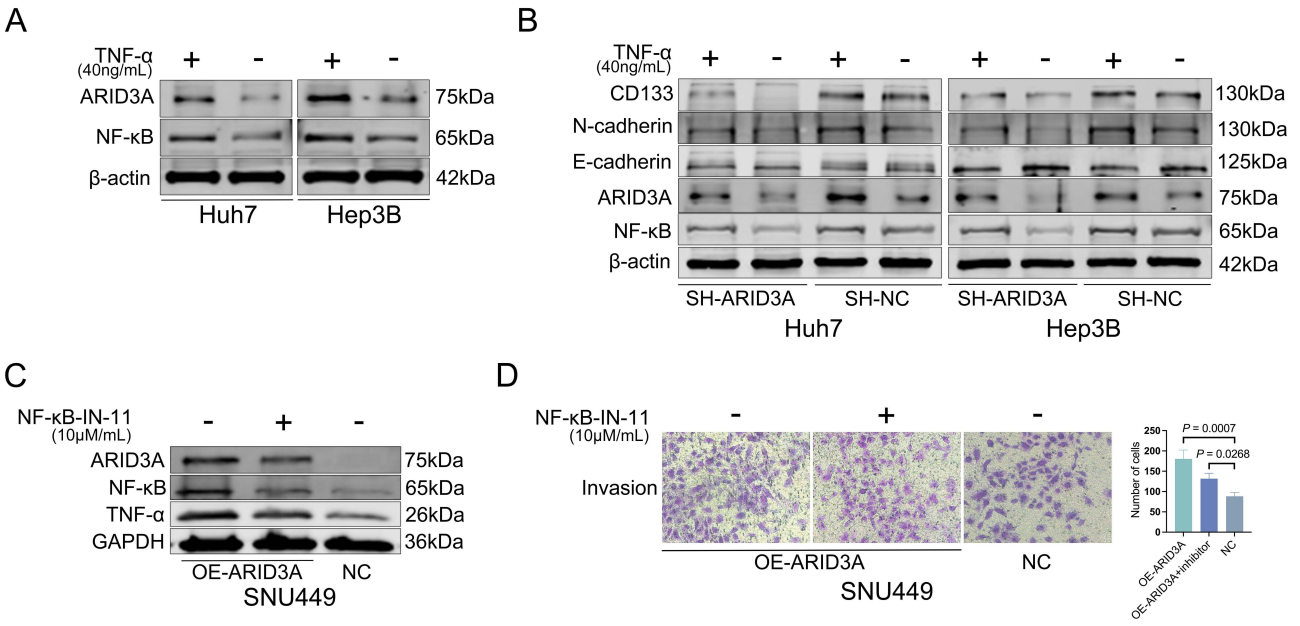

Figure 6 ARID3A promotes stemness and mesenchymal phenotype of HCC cell lines via TNF-α-mediated NF-κB pathway.(**A** and **B**) TNF-α activated NF-κB signaling and promoted ARID3A expression in both wild-type (**A**) and ARID3A lentivirus-transfected (**B**) Huh7 and Hep3B cells (n = 3). (**C**) The expression of ARID3A, NF-κB and TNF-α was reduced in SNU449 cells after treated with NF-κB inhibitor (n = 3). (**D**) Inhibition of NF-κB signaling restrained the ARID3A-induced invasive ability of SNU449 cells (n = 3).

reversed the inhibition of ARID3A and NF-κB expression, as well as that of CSC and EMT markers (Figure 6B). Subsequently, we also conducted the blocking experiment of NF-κB signaling using NF-κB-IN-11, a specific inhibitor of TNF-α-mediated NF-κB signaling. The expression of ARID3A and TNF-α decreased after NF-κB inhibition in SNU449 cells (Figure 6C). Meanwhile, NF-κB inhibition also restrained the invasiveness of SNU449 cells after ARID3A overexpression (Figure 6D). These results demonstrated that ARID3A regulated tumor stemness and invasiveness by activating TNF-α-mediated NF-κB signaling.

Discussion

The initiation and regulatory mechanisms of the strong CSC characteristics and aggressive phenotypes in DPHCC have not been fully elucidated. In the present study, we conducted RNA-seq analyses on DPHCC and found that the transcription factor ARID3A was upregulated and might serve as a potential regulator of stemness features in DPHCC. In vitro and in vivo assays suggested that ARID3A enhanced tumor stemness and promoted invasive ability of HCC cells. Transcriptional activation of ARID3A has been reported in several malignancies.[13,14,19] ARID3A regulates the expression of stemness markers and facilitates the CSC phenotype in ovarian cancer by activating several oncogenic pathways.[13] Similarly, a previous study suggested that ARID3A enhanced tumor stemness by modulating the transcriptional regulation process,[15] which was consistent with the result of KEGG analysis of DPHCC-related genes suggesting that these genes were implicated in the transcriptional regulation of the RNA polymerase II promoter.

The RNA-seq of ARID3A-transfected cells revealed that the oncogenic potential of ARID3A was involved in the activation of TNF-α-mediated NF-κB signaling. KEGG analyses also indicated that ARID3A was involved in the regulatory process of TNF-α-mediated inflammatory response. The correlation between inflammatory signaling and tumor stemness have been validated in numerous malignancies.[20,21] The proinflammatory factors TNF-α and IL-6 can be released by the inflammatory niche, and thereby promoting tumor stemness and activating the EMT programme.[22,23] The disparity between CSCs and bulk malignant cells may result mainly from EMT activation.[24,25] Interestingly, our results also suggested that the ARID3A expression could also be induced by TNF-α, thereby leading to the activation of the EMT programme. Similar to ARID3A, its paralogue gene ARID3B can also induce TNF-α expression and is involved in the TNF-α-mediated signaling.[26] Although TNF-α is generally considered a proinflammatory cytokine, emerging

evidence indicates that it plays a crucial role in regulating tumor stemness. TNF-α not only induces EMT by activating the NF-κB signaling,[27,28] but also induces the CSC phenotype through the non-canonical NF-κB pathway.[29] Previous studies have shown that the TNF-α/NF-κB signaling is essential for facilitating tumor invasion and metastasis.[30] Activation of NF-κB signaling can promote the invasion and metastatic ability of tumor cells.[8,30,31] In vitro blocking of TNF-α-mediated NF-κB signaling suppressed the invasive ability of HCC cells further emphasized the important role of NF-κB signaling in ARID3A-induced invasiveness. These results collectively indicated that the upregulated expression of ARID3A in DPHCC might lead to the activation of several oncogenic signaling pathways associated with inflammation, which might confer CSC potential to DPHCC and maintain its stemness.

Several limitations should be noted in our study: Firstly, the transcriptomic information from HCC cohort should be cautiously interpreted, as the sample size of this cohort was relatively small and lacked of validation cohort. Then, the findings of our study may require more in-depth in vitro assays or orthotopic mouse models to validate the therapeutic efficacy of targeting the ARID3A–TNF-α/NF-κB axis.

In conclusion, our study revealed that ARID3A might be a potential regulator of inflammation-induced tumor stemness and invasiveness in DPHCC. Inhibition of ARID3A-mediated TNF-α/NF-κB signaling may be a potential target for cancer therapy in future directions.

Data Sharing Statement

The RNA-seq data are available from the corresponding author (Bangde Xiang) upon reasonable request.

Ethics Statement

This study was approved by the Ethics Committee of Guangxi Medical University Cancer Hospital (NO. KY2025049). Preoperative informed consent was obtained from all the patients in the RNA-seq cohort. Animal experiments were conducted in accordance with the ethical and legal regulations and were also approved by the Animal Center of Guangxi Medical University.

Author Contributions

All authors made a significant contribution to the work reported, whether that is in the conception, study design, execution, acquisition of data, analysis and interpretation, or in all these areas; took part in drafting, revising or critically reviewing the article; gave final approval of the version to be published; have agreed on the journal to which the article has been submitted; and agree to be accountable for all aspects of the work.

Funding

This research was supported by the National Natural Science Foundation of China (82260573), Innovation Project of Guangxi Graduate Education (YCBZ2025109), the Key Laboratory of Early Prevention and Treatment for Regional High Frequency Tumor (Guangxi Medical University), Ministry of Education (GKE-ZZ202215 and GKE-ZZ202315). The Science and Technology Program of Fangchenggang (Fangke AB23006028).

Disclosure

The authors declare no conflicts of interest in this work.

References

1. Reig M, Forner A, Rimola J, et al. BCLC strategy for prognosis prediction and treatment recommendation: the 2022 update. *J Hepatol*. 2022;76(3):681–693.
2. Lee TK, Guan XY, Ma S. Cancer stem cells in hepatocellular carcinoma - from origin to clinical implications. *Nat Rev Gastroenterol Hepatol*. 2022;19(1):26–44. doi:10.1038/s41575-021-00508-3
3. Lu XY, Xi T, WY L, et al. Hepatocellular carcinoma expressing cholangiocyte phenotype is a novel subtype with highly aggressive behavior. *Ann Surg Oncol*. 2011;18(8):2210–2217. doi:10.1245/s10434-011-1585-7
4. Govaere O, Komuta M, Berkers J, et al. Keratin 19: a key role player in the invasion of human hepatocellular carcinomas. *Gut*. 2014;63(4):674–685. doi:10.1136/gutjnl-2012-304351
5. Lee CW, Kuo WL, Yu MC, et al. The expression of cytokeratin 19 in lymph nodes was a poor prognostic factor for hepatocellular carcinoma after hepatic resection. *World J Surg Oncol*. 2013;11(1):136. doi:10.1186/1477-7819-11-136

6. Marquardt JU, Gomez-Quiroz L, Arreguin Camacho LO, et al. Curcumin effectively inhibits oncogenic NF-kappaB signaling and restrains stemness features in liver cancer. *J Hepatol*. 2015;63(3):661–669. doi:10.1016/j.jhep.2015.04.018
7. Yang XR, Xu Y, Yu B, et al. High expression levels of putative hepatic stem/progenitor cell biomarkers related to tumour angiogenesis and poor prognosis of hepatocellular carcinoma. *Gut*. 2010;59(7):953–962. doi:10.1136/gut.2008.176271
8. Zhao Z, Sun H, Liu Y, et al. PDPN+ cancer-associated fibroblasts enhance gastric cancer angiogenesis via AKT/NF-kappaB activation and the CCL2-ACKR1 axis. *MedComm*. 2025;6(1):e70037. doi:10.1002/mco2.70037
9. Kaltschmidt C, Banz-Jansen C, Benhidjeb T, et al. A Role for NF-kappaB in organ specific cancer and cancer stem cells. *Cancers*. 2019;11(5):655. doi:10.3390/cancers11050655
10. Lei ZN, Teng QX, Koya J, et al. The correlation between cancer stem cells and epithelial-mesenchymal transition: molecular mechanisms and significance in cancer theragnosis. *Front Immunol*. 2024;15:1417201.
11. Parlayan C, Sahin Y, Altan Z, Arman K, Ikeda MA, Saadat K. ARID3A regulates autophagy related gene BECN1 expression and inhibits proliferation of osteosarcoma cells. *Biochem Biophys Res Commun*. 2021;585:89–95. doi:10.1016/j.bbrc.2021.11.035
12. Patsialou A, Wilsker D, Moran E. DNA-binding properties of ARID family proteins. *Nucleic Acids Res*. 2005;33(1):66–80. doi:10.1093/nar/gki145
13. Dausinas P, Pulakanti K, Rao S, Cole JM, Dahl R, Cowden Dahl KD. ARID3A and ARID3B induce stem promoting pathways in ovarian cancer cells. *Gene*. 2020;738:144458. doi:10.1016/j.gene.2020.144458
14. Wang J, Rao S, Chu J, et al. A protein interaction network for pluripotency of embryonic stem cells. *Nature*. 2006;444(7117):364–368. doi:10.1038/nature05284
15. Shen M, Li S, Zhao Y, et al. Hepatic ARID3A facilitates liver cancer malignancy by cooperating with CEP131 to regulate an embryonic stem cell-like gene signature. *Cell Death Dis*. 2022;13(8):732. doi:10.1038/s41419-022-05187-9
16. Li S, Wu Z, Li Q, et al. The Prognostic Value of AT-Rich Interaction Domain (ARID) family members in patients with hepatocellular carcinoma. *Evid Based Complement Alternat Med*. 2022;2022:1150390. doi:10.1155/2022/1150390
17. Yang CL, Qiu X, Lin JY, et al. Potential role and clinical value of PPP2CA in hepatocellular carcinoma. *J Clin Transl Hepatol*. 2021;9(5):661–671. doi:10.14218/JCTH.2020.00168
18. Zhang J, Qi YP, Ma N, et al. Overexpression of epcam and cd133 correlates with poor prognosis in dual-phenotype hepatocellular carcinoma. *J Cancer*. 2020;11(11):3400–3406. doi:10.7150/jca.41090
19. Tang J, Yang L, Li Y, et al. ARID3A promotes the development of colorectal cancer by upregulating AURKA. *Carcinogenesis*. 2021;42(4):578–586. doi:10.1093/carcin/bgaa118
20. Briede I, Balodis D, Gardovskis J, Strumfa I. Stemness, inflammation and epithelial-mesenchymal transition in colorectal carcinoma: the intricate network. *Int J Mol Sci*. 2021;22(23):12891. doi:10.3390/ijms222312891
21. Liu Y, Xu Q, Deng F, et al. HERC2 promotes inflammation-driven cancer stemness and immune evasion in hepatocellular carcinoma by activating STAT3 pathway. *J Exp Clin Cancer Res*. 2023;42(1):38. doi:10.1186/s13046-023-02609-0
22. Chen Y, Wen H, Zhou C, et al. TNF-alpha derived from M2 tumor-associated macrophages promotes epithelial-mesenchymal transition and cancer stemness through the Wnt/beta-catenin pathway in SMMC-7721 hepatocellular carcinoma cells. *Exp Cell Res*. 2019;378(1):41–50. doi:10.1016/j.yexcr.2019.03.005
23. Sullivan NJ, Sasser AK, Axel AE, et al. Interleukin-6 induces an epithelial-mesenchymal transition phenotype in human breast cancer cells. *Oncogene*. 2009;28(33):2940–2947. doi:10.1038/onc.2009.180
24. Polyak K, Weinberg RA. Transitions between epithelial and mesenchymal states: acquisition of malignant and stem cell traits. *Nat Rev Cancer*. 2009;9(4):265–273. doi:10.1038/nrc2620
25. Shibue T, Weinberg RA. EMT, CSCs, and drug resistance: the mechanistic link and clinical implications. *Nat Rev Clin Oncol*. 2017;14(10):611–629. doi:10.1038/nrclinonc.2017.44
26. Joseph S, Deneke VE, Cowden Dahl KD. ARID3B induces tumor necrosis factor alpha mediated apoptosis while a novel ARID3B splice form does not induce cell death. *PLoS One*. 2012;7(7):e42159. doi:10.1371/journal.pone.0042159
27. Min C, Eddy SF, Sherr DH, Sonenshein GE. NF-kappaB and epithelial to mesenchymal transition of cancer. *J Cell Biochem*. 2008;104(3):733–744. doi:10.1002/jcb.21695
28. Wu Y, Deng J, Rychahou PG, Qiu S, Evers BM, Zhou BP. Stabilization of snail by NF-kappaB is required for inflammation-induced cell migration and invasion. *Cancer Cell*. 2009;15(5):416–428. doi:10.1016/j.ccr.2009.03.016
29. Liu W, Lu X, Shi P, et al. TNF-alpha increases breast cancer stem-like cells through up-regulating TAZ expression via the non-canonical NF-kappaB pathway. *Sci Rep*. 2020;10(1):1804. doi:10.1038/s41598-020-58642-y
30. Wu Y, Zhou BP. TNF-alpha/NF-kappaB/Snail pathway in cancer cell migration and invasion. *Br J Cancer*. 2010;102(4):639–644. doi:10.1038/sj.bjc.6605530
31. Wu TJ, Chang SS, Li CW, et al. Severe hepatitis promotes hepatocellular carcinoma recurrence via nf-kappab pathway-mediated epithelial-mesenchymal transition after resection. *Clin Cancer Res*. 2016;22(7):1800–1812. doi:10.1158/1078-0432.CCR-15-0780